Available online at www.sciencedirect.com
SCIENCE DIRECT®
Pergamon
Cement and Concrete Research 34 (2004) 1389–1402
CEMENT AND CONCRETE RESEARCH

Alkali–silica reactivity of large silica fume-derived particles

M.C.G. Juenger[a,*], C.P. Ostertag[b]

[a]Department of Civil Engineering, University of Texas, Austin, TX 78712, USA
[b]Department of Civil and Environmental Engineering, University of California, Berkeley, CA 94270, USA

Received 22 July 2002; accepted 2 January 2004

Abstract

Pozzolanic materials, including silica fume, are commonly added to concrete to reduce expansion due to alkali–silica reaction (ASR). It has been noted, however, that commercial silica fume is not always adequately dispersed, and large agglomerates may be present. These large particles have been hypothesized to act as amorphous silica aggregates, thereby participating in an expansive reaction with the alkalis present in cement paste pore solution. If such were the case, some silica fume particles would actually aggravate expansion due to ASR rather than suppress it. The present investigation characterizes the microstructure and morphology of agglomerated and sintered silica fume particles and compares their effects on alkali–silica-related expansion. While a 5% replacement of moderately reactive sand with sintered silica fume aggregates caused significant expansion under accelerated testing conditions (modified ASTM C1260), the replacement with large agglomerates of densified silica fume decreased expansion compared with control mortar bars containing only sand. Both the sintered aggregates and the agglomerates reacted with the pore solution; one reaction was expansive, while the other was not.

Keywords: Microstructure; Alkali-aggregate reaction; Expansion; Silica fume

1. Introduction

It is well known that the replacement of a small percentage of cement with a pozzolanic material reduces the expansion that occurs when alkali hydroxides react with silica-containing aggregates. The means by which this is accomplished is unresolved, yet, several theories have been presented. The most commonly discussed mechanisms are the following [1]: (a) pozzolans reduce permeability, thereby preventing the ingress of water and transport of alkali and hydroxyl ions; (b) pozzolans increase strength and stiffness, resulting in better resistance to cracking and less expansion; (c) replacing a portion of cement with a less-alkaline pozzolanic material decreases the total amount of alkali present; and (d) pozzolans react with calcium hydroxide (CH) to form calcium silicate hydrate (C–S–H) with a low CaO/SiO_2 (C/S) ratio. Formation of this C–S–H depletes CH and the low C/S ratio enables the entrapment of alkalis, both of which reduce the amount of hydroxyl ions available to participate in the alkali–silica reaction (ASR).

Silica fume, with particle sizes averaging 0.1 μm in diameter, is commonly used in structural concrete and can be used to control expansion due to ASR. However, it has recently been documented that many commercial silica fumes contain a portion of very coarse particles (larger than 100 μm) [2,3]. Silica fume is generally transported in densified or pelletized form. The pelletized version is intended to be interground with cement prior to use; if not, very large pellets are certain to be present. Agglomerates in densified silica fume are assumed to be broken apart during concrete mixing, but are sometimes intact in hardened concrete [4,5]. The microstructure of such silica fume agglomerates has been addressed by several researchers (e.g., Refs. [2,3,5,6]). It has been observed that the agglomerates can be quite dense [2,5] and may be held together by van der Waals forces [6] and/or by entangled chains of silica fume [7]. It has been suggested that agglomerates or large siliceous particles in silica fume behave as small aggregates, rather than as pozzolans, and react expansively with alkalis in cement [8].

Several examinations have been done, both in the laboratory and in the field, to determine whether large particles

* Corresponding author. Tel.: +1-512-232-3593; fax: +1-512-471-7259.
E-mail address: mjuenger@mail.utexas.edu (M.C.G. Juenger).

0008-8846/$ – see front matter © 2004 Elsevier Ltd. All rights reserved.
doi:10.1016/j.cemconres.2004.01.001

in silica fume participate deleteriously in ASR. The first quantitative evidence for silica fume participating in ASR comes from a laboratory study by Perry and Gillott [9]. They showed that at replacement levels greater than 20%, silica fume eliminated expansion caused by 4% opal. Replacement of 5% of the cement by silica fume actually increased expansion in those tests that were accelerated by increasing the temperature. Shayan et al. [10,11] showed that a 20% replacement of cement by densified silica fume significantly reduced expansion when reactive aggregates were used. When nonreactive basalt aggregates were used, the authors saw a very slight increase in expansion due to the silica fume. Rangaraju and Olek [12] saw increases in the expansion of cement paste prisms containing 10% agglomerated silica fume under accelerated testing conditions.

Another laboratory test by Pettersson [13] showed an increase in cracking in mortar bars containing 10% compacted silica fume compared with dispersed silica fume. The cracks were shown to originate around the silica fume granules, and alkali–silica gel was present. However, no quantitative data confirming an increase in expansion were presented, and it is not clear whether the aggregates used were reactive. St. John and Freitag [14] saw increases in cracking in structures containing undispersed silica fume. Likewise, Marusin and Shotwell [15] documented cracking in a structure containing silica fume agglomerates, that had reacted with the pore solution.

On the other hand, Gundmundsson and Olafsson [4] reported that, although large clusters of silica fume were present in the cores taken from several structures, there was no evidence of ASR occurring in these regions. Furthermore, extensive laboratory testing by Boddy et al. [16], comparing slurried, densified, and pelletized forms of silica fume, showed that all forms of silica fume (at cement replacement levels of 8% and 12%) reduced expansion due to ASR when reactive aggregates were used.

The evidence for silica fume agglomerates participating in ASR is therefore inconclusive. The discrepancies in the literature may arise from differences in testing methods or from differences in materials. The current investigation was undertaken to explore further the effects of various forms of silica fume on ASR. In this case, silica fume was treated as an aggregate, rather than as a replacement of cement. Agglomerates, sieved from a barrel of commercial densified silica fume, were compared with silica fume that had been sintered to bond the individual particles together. The silica fume was added as a 5% replacement of the aggregate by mass in mortar, with the remainder of the aggregate composed of either reactive sand or nonreactive limestone. The samples were measured for ASR expansion under accelerated testing conditions. The morphology, microstructure, and composition of the silica fume agglomerates and aggregates were examined before and after expansion testing using optical microscopy, scanning electron microscopy, and electron probe microanalysis.

2. Experimental

2.1. Silica fume preparation

Agglomerates were dry-sieved from a barrel of a widely used, commercially available, densified silica fume. Three size ranges of agglomerates were used. The smallest size range, designated "fine", was passed through a #200 sieve, and all agglomerates were therefore less than 75 μm. The "medium"-sized particles were passed through a #50 sieve and retained on a #200 sieve (75–300 μm). "Large" refers to particles in the size range and gradation of aggregates specified by ASTM C1260 [17], with sizes ranging from 150 μm to 4.75 mm (#100–#4 sieve sizes).

Synthetic aggregates were made by applying a pressure of 72 MPa onto a 50 × 50 mm steel mold containing 10-g batches of silica fume [the silica fume passed a #30 size sieve (600 μm) prior to pressing]. The pellets were heated in a laboratory muffle furnace to 1000 °C and maintained at this temperature for 1 h. They were then allowed to cool slowly in the furnace to 700 °C, at which point the pellets were removed from the furnace and allowed to cool at room temperature. The sintered pellets were broken with a hammer to particle sizes between 4.75 and 150 μm (passing through #4 size sieve and retained on #100 size sieve). X-ray diffraction analysis showed that the silica in the aggregates, before and after sintering, was entirely amorphous.

2.2. Silica fume characterization

The microstructure of the silica fume agglomerates and sintered aggregates was assessed using a scanning electron microscope (SEM; JSM-6300, JEOL, Peabody, MA), in secondary electron imaging (SE) mode. Several particles of each type were dried under vacuum. These were then impregnated under vacuum with an ultra-low viscosity epoxy. Prior to analysis by SEM, the samples were polished to 1/4 μm and coated with a thin layer of gold-palladium.

Silica fume agglomerates and aggregates were also mixed in mortar specimens to assess their reactivity with cement paste and expansion due to ASR (details of the mortar bar preparation and expansion test are in the next section). Cross-sections (12 mm) of the mortar bars were taken after curing for 1, 2, and 7 days (prior to NaOH exposure) and after 39 days of expansion testing for examination with an optical microscope. The cross-sections were polished to 3 μm and were kept moist during preparation and observation.

Cross-sections (2 mm) of samples after 7 days of curing and after 39 days of expansion testing were examined with an electron microprobe (SX-51, Cameca Instrument, Trumbull, CT). The sample preparation was identical with that described above for SEM, but the samples were coated with carbon instead of gold-palladium. Backscattered electron (BSE) images were taken of several locations. Quantitative

elemental analysis was also performed over selected areas, in 5-μm spots, using a wavelength dispersive spectrometer (WDS).

2.3. ASR expansion

Expansion studies were performed according to a modification of the method outlined in ASTM C1260 [17]. This test, also known as the accelerated mortar-bar method, has been shown to be effective in determining the ability of pozzolans to reduce expansion due to ASR [18,19]. It involves submerging mortar bars in 1 N NaOH solution at 80 °C, after curing for 1 day at 20 °C and 1 day underwater at 80 °C. The technique was modified by extending the underwater curing period at 80 °C from 1 to 6 days; thus, the results are comparable with those from other previous and concurrent studies [20,21]. For each set of parameters examined, two batches of three mortar bars each were tested.

ASTM Type I/II Portland cement with Na_2O equivalent $<0.6\%$ and two types of aggregates were used: sand and nonreactive limestone. The naturally occurring sand was composed primarily of aphanite, quartz, gneiss, and granite, with some sandstone and metavolcanic material. The limestone aggregates were crushed from a flooring tile of Jerusalem limestone. The water-to-cement ratio was 0.47, and the aggregate-to-cement ratio was 2.25 by mass, as specified by ASTM C1260 [17]. To test whether large silica fume particles act as reactive aggregates, 5% of the aggregate by mass was replaced by silica fume in various size ranges. The replacement value of 5% was chosen because it has been shown to be the "pessimum" proportion for many reactive aggregates [22]. Silica fume agglomerates were used in the three different size ranges described in Section 2.1: fine, medium, and large. It was expected that some, but not all, of these particles would break apart upon mixing. Sintered silica fume aggregates in the *large* size range were also tested for expansion, and were also used as a 5% replacement of sand by mass.

3. Results

3.1. Silica fume microstructure

SE images of silica fume agglomerates are shown in Figs. 1 and 2. The agglomerate in Fig. 1a clearly has distinct outer and inner regions. With higher magnification (Fig. 1b–d), it can be seen that the outer region consists of small, individual spheres of silica fume that are more closely packed than in the center. The spheres are heterogeneously

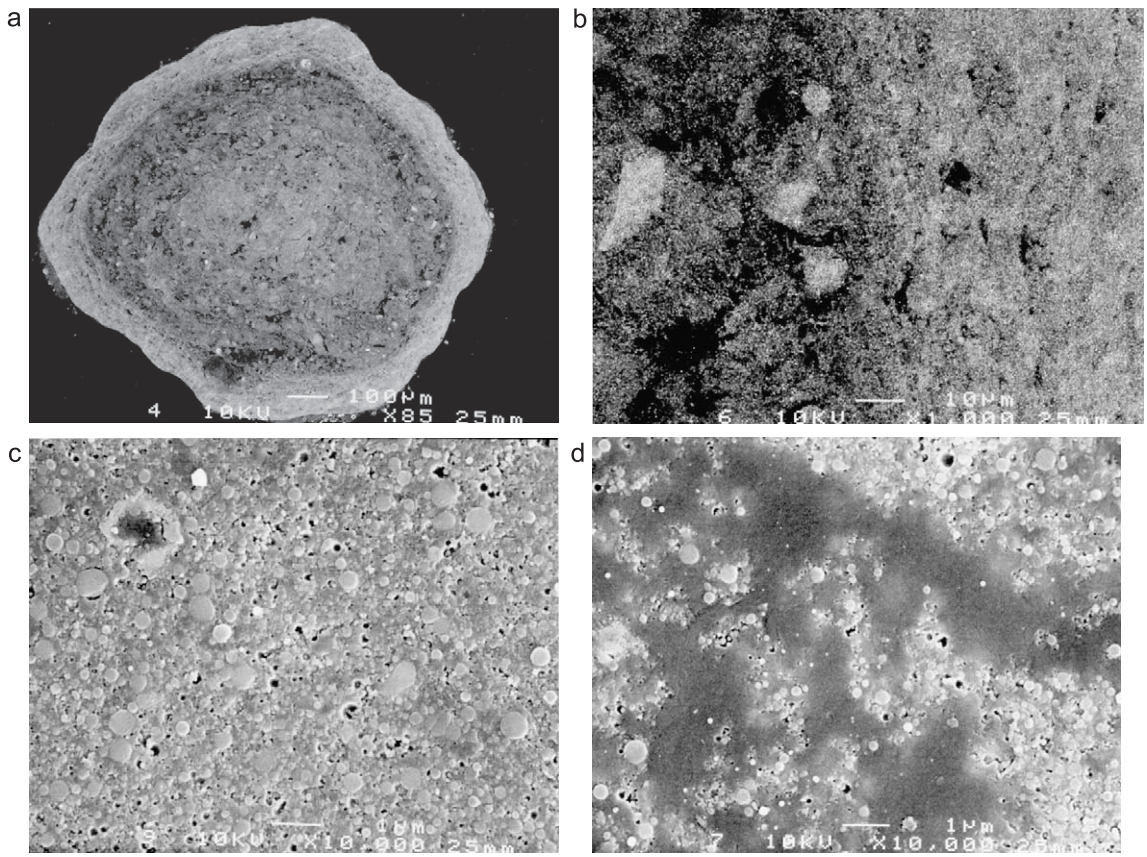

Fig. 1. SE images of an epoxy-impregnated, polished cross-section of a silica fume agglomerate sieved from a barrel of densified silica fume: (a) full agglomerate, (b) magnified area, (c) high-density outer area, higher magnification, and (d) low-density central area. Darker regions are epoxy-filled spaces.

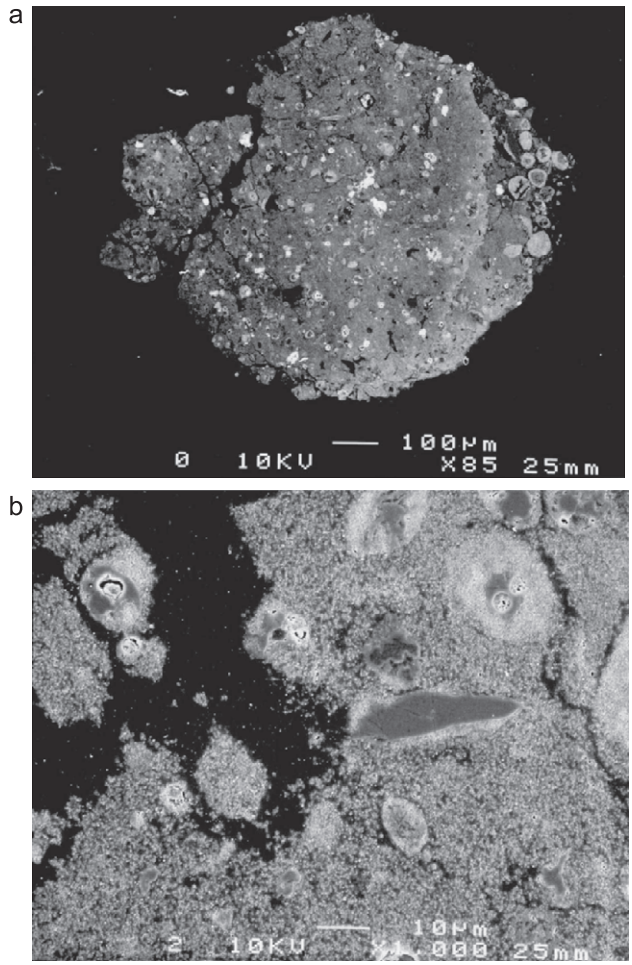

Fig. 2. SE images of an epoxy-impregnated, polished cross-section of a silica fume agglomerate sieved from a barrel of densified silica fume: (a) full agglomerate and (b) magnified area.

distributed in the central region, with areas of close packing and empty channels (Fig. 1d). Fig. 2 shows another agglomerate with a different morphology. This agglomerate contains many more impurities (Fig. 2a); yet, with higher magnification (Fig. 2b), the silica fume particles closely resemble those in Fig. 1. Among those studied, there were several agglomerates of both types, with varying sizes.

Fig. 3 shows SE images of a cross-section of a sintered silica fume aggregate. The microstructure is strikingly different from the agglomerate in that necks have formed between the silica fume particles during the sintering process, creating a much denser aggregate. There are still some discrete pores, and there are only a few bright individual particles that have not been incorporated into the dense matrix (Fig. 3b).

3.2. Silica fume in mortar

3.2.1. Agglomerates

Fig. 4 shows optical microscope images of silica fume agglomerates in mortar cured at 20 °C for 24 h. The agglomerates are light gray and uniform in color, but have a rough texture and are sometimes hollow (Fig. 4a). Many agglomerates remain intact after mixing, and some are quite large, on the order of several hundred micrometers. Because the silica fume particles are only weakly held together, they can be easily disturbed by the polishing process, resulting in rough surfaces and hollow interiors. Since many agglomerates are less dense in the center (Fig. 1a), and these samples have not been impregnated with epoxy, the interiors more easily dispersed when they are sliced open and polished. It is also possible that some agglomerates are originally hollow, having only a densely packed outer shell.

Further curing significantly changes the appearance of the silica fume agglomerates (Fig. 5). One additional day of curing at 80 °C results in a two-toned morphology of the larger agglomerates, as seen in Fig. 5a. The agglomerates have white interiors and dark gray exterior rims. Longer curing at 80 °C causes no further changes (Fig. 5b). The centers of these large agglomerates are all either completely hollow or contain small, empty pockets. This morphology

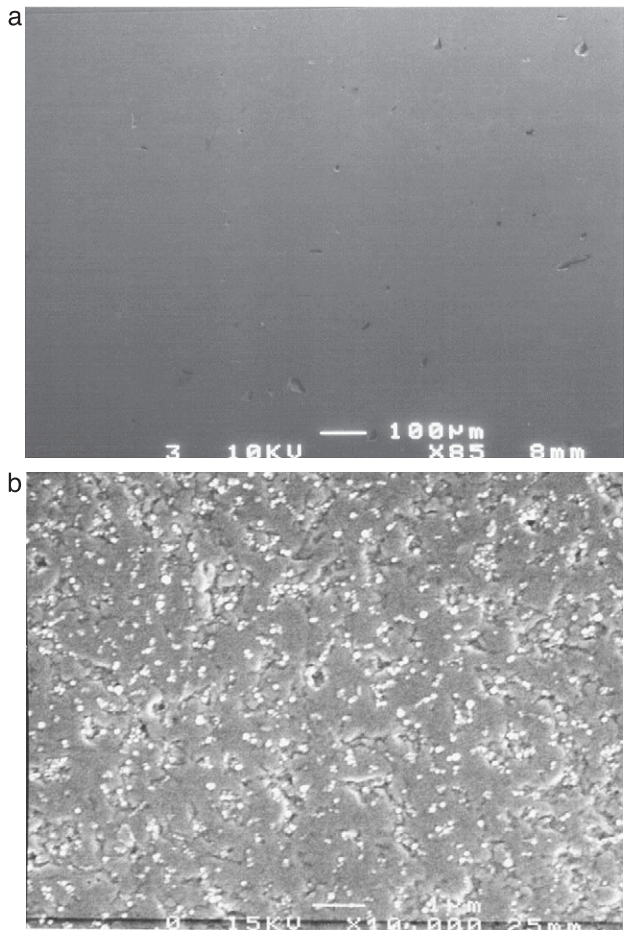

Fig. 3. SE images of an epoxy-impregnated, polished cross-section of a sintered silica fume aggregate: (a) center of aggregate and (b) magnified area.

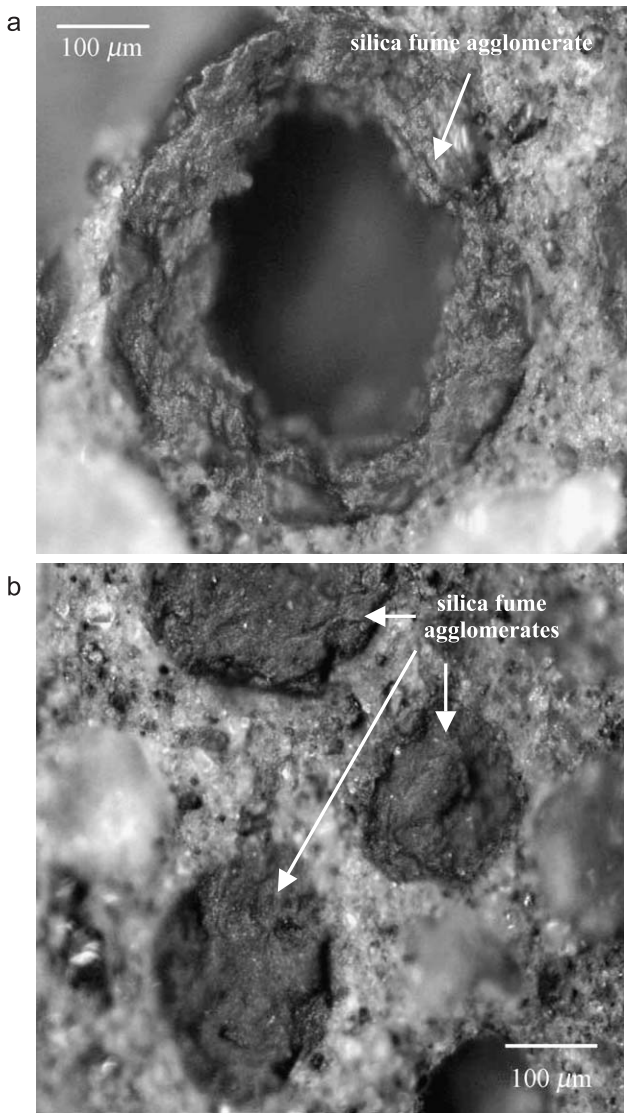

Fig. 4. Optical microscope images of silica fume agglomerates in mortar, cured for 24 h at 20 °C.

is probably a result of the original low density of the agglomerates. More interesting is the two-toned coloration. The area close to the cement paste seems to be much darker and denser compared with the agglomerates in Fig. 4, while the interior is lighter. The color change is not the result of moisture gradients in the sample, as the appearance does not change with vacuum drying. The color change is also not an artifact of high temperature curing, as it also appears in specimens cured for 6 months at room temperature. The two-toned appearance is independent of the reactivity of the remainder of the aggregates, i.e., sand or limestone.

Another interesting feature of extended curing is the change in the smaller agglomerates (< 100 μm). There are some of these in Fig. 5b, all of them uniformly dark. The lighter interior rim and hollow centers are conspicuously missing. A likely explanation for the change in morphology with extended curing is that the silica fume agglomerates are reacting with the cement paste. The smaller agglomerates react throughout, while the larger ones only react in the regions closest to the paste. The mortar samples were studied further using an electron microprobe to investigate this possibility.

Table 1 shows data from an electron probe microanalysis (EPMA) of silica fume agglomerates and sintered aggregates in mortar, before and after exposure to the 1 N NaOH solution at 80 °C. The average values were calculated using data from approximately 50–100 points (each) across many agglomerates and aggregates. The terms "interior" and "exterior" refer to the zones of the aggregates appearing as different colors or porosities in optical and/or BSE

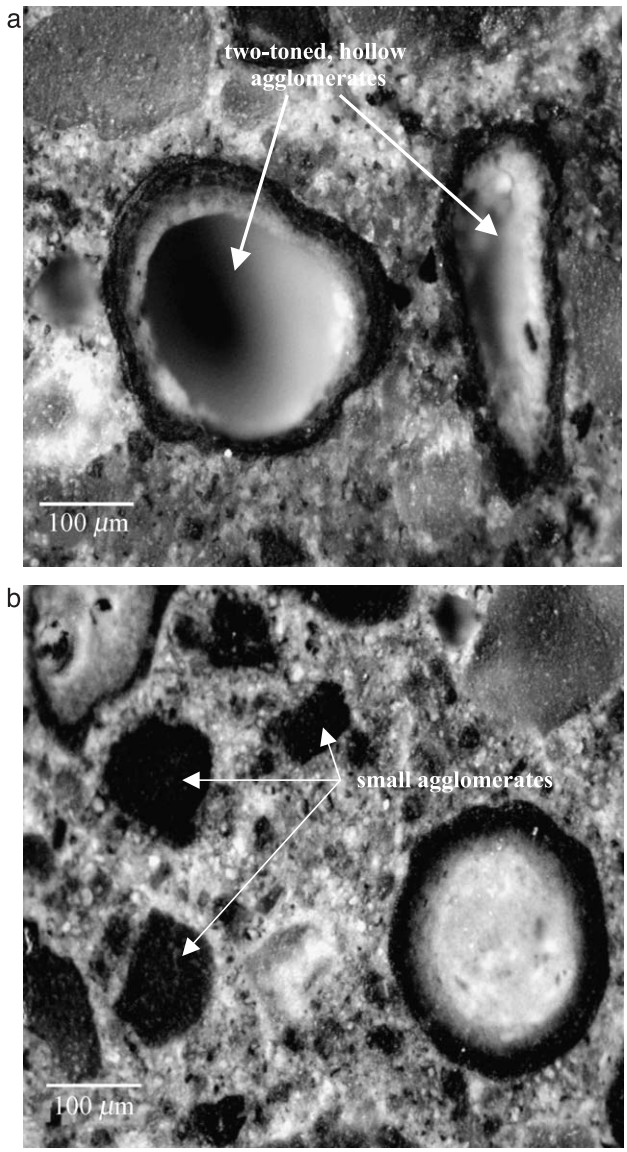

Fig. 5. Optical microscope images of silica fume agglomerates in mortar: (a) cured 24 h at 20 °C + 24 h at 80 °C and (b) cured 24 h at 20 °C + 6 days at 80 °C.

Table 1
Electron probe microanalysis data from several points (oxide percent)

			SiO_2	CaO	Na_2O	CaO/SiO_2	Total
Silica fume agglomerates	Interior	Average	42	3.5	0.64	0.09	44
		Range	20–76	1.0–8.4	0.00–1.7	0.03–0.26	17–74
	Exterior	Average	72	11	1.0	0.15	86
		Range	59–81	5.6–20	0.12–1.9	0.08–0.32	74–93
Sintered silica fume	Interior	Average	84	0.38	0.15	0.00	80
		Range	77–96	0.23–1.2	0.10–0.30	0.00–0.01	74–86
	Exterior	Average	87	2.8	0.32	0.03	88
		Range	74–95	1.4–6.8	0.18–0.53	0.02–0.08	78–93
Silica fume agglomerates (after NaOH exposure)	Interior	Average	57	19	6.9	0.33	91
		Range	50–66	12–25	0.77–22	0.20–0.46	81–103
	Exterior	Average	45	20	11	0.46	82
		Range	35–72	15–27	2.8–23	0.22–0.71	75–101
Sintered silica fume (after NaOH exposure)	Interior	Average	28	10	3.6	0.36	44
		Range	20–36	7–14	2.1–4.3	0.29–0.57	32–57
	Exterior	Average	52	23	8.0	0.44	97
		Range	47–57	20–26	2.9–12	0.39–0.50	91–101

images. The term ‘‘total’’ refers to how much, in the particular spot being examined, can be accounted for by the elements analyzed. A value less than 100% indicates that the area is either porous or contains a significant amount of chemically bound water, neither of which can be detected by EPMA. The values for SiO_2, CaO, and Na_2O in Table 1 do not necessarily add up to the total, as other oxides were also analyzed, which were not relevant to this discussion and whose values are not presented (Al_2O_3, FeO, MnO, and MgO).

From Table 1, it appears that, on average, the interior of silica fume agglomerates is much more porous than the exterior, with totals of 44% compared with 86%, respectively. The interior may contain less calcium. However, these numbers are deceiving because the values for the individual oxides are correlated with those of the totals; the values for individual oxides increase or decrease with the totals.

While the data in Table 1 represent averages over several particles, EPMA data were also collected on linear traverses through the particle of interest. A BSE image of a large silica fume agglomerate in mortar, cured at 20 °C for 1 day and at 80 °C for 6 days, is shown in Fig. 6a. This specimen is characteristic of large agglomerates in that the center appears to be very porous. A plot of the composition along a line traversing the agglomerate, as measured by EPMA, is shown in Fig. 6b. The gaps in the plots are areas where the points examined by EPMA were on the interface between the cement paste matrix and the agglomerate; points at interfaces are often misleading and were therefore omitted. It is clear from the drop in the totals in the center of the agglomerate in Fig. 6b that the center is very porous. From an examination of the BSE image in Fig. 6a and the totals in Fig. 6b, there appear to be three discrete regions in the agglomerate: an exterior, very dense rim, an interior, less dense rim, and a porous center.

If the agglomerate does not react with the cement paste, the lines for SiO_2 and totals should almost overlap, as the original agglomerate is over 90% silica. This is not the case in Fig. 6b, as the amount of SiO_2 is, on average, 20% less than the total. It appears from both Fig. 6 and Table 1 that a significant amount of calcium can be found within the agglomerate. In Fig. 6c, the *y*-axis scale of the plot from Fig. 6b has been reduced so that the amount of CaO in this agglomerate can be seen more clearly. The amounts range from 4% to 14%, with higher concentrations near the agglomerate/paste interface. The decrease in CaO toward the center is confounded with the decrease in the total amount of oxides detected by EPMA, so it is difficult to tell from these data if the amount of calcium decreases with the distance from the paste.

The amount of Na_2O is also shown in Fig. 6b and c. The amount of alkalis, both Na_2O and K_2O (not shown), does not change much through the agglomerate and paste, nor are the concentrations very high, never exceeding 2%. It appears from Fig. 6c that, perhaps, the concentration of Na_2O is higher near the edge of the agglomerate. However, it is difficult to make conclusions from these data because the concentrations are so small and these fluctuations track with the totals. Data for Na_2O in Table 1 show that there is no discernable difference in the amounts of sodium in the interior compared with the exterior of the agglomerates.

3.2.2. Sintered aggregates

An example of a sintered silica fume aggregate in mortar, after curing at 80 °C and prior to expansion testing, is shown in Fig. 7. These aggregates have a uniform, smooth texture and are light gray or white in color. Fig. 8a shows a BSE image of a portion of a sintered silica fume aggregate in mortar, prior to NaOH exposure, and of the oxide analyses of points taken across the aggregate. This particular aggregate is very large, and the interior appears to be slightly darker than the part close to the cement paste. The bicoloration is most likely related to impurities. This particular aggregate appears white in

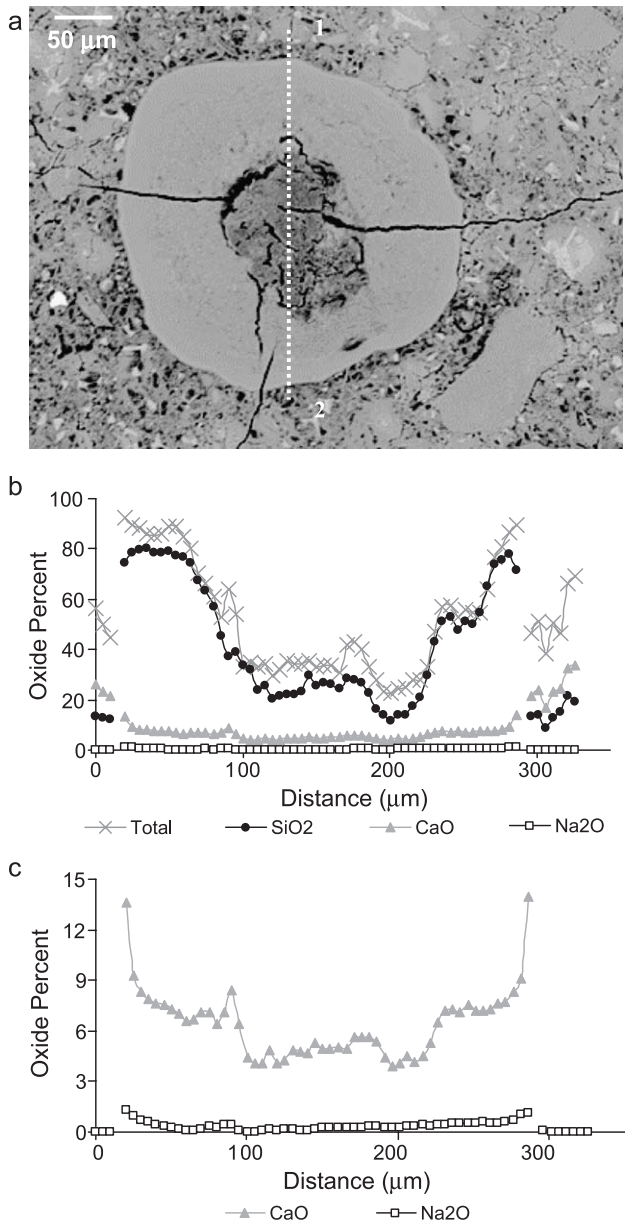

Fig. 6. (a) BSE image of a silica fume agglomerate. (b) Elemental composition along the dotted line in Panel (a) from Point 1 to 2. (c) Same plot as in Panel (b), but with reduced *y*-axis scale.

the center and light gray at the rim in an optical microscope. The silica fume used to produce the aggregates was originally dark gray and turned white after sintering; impurities are burned off during sintering, resulting in a color change. Some areas of the pellet remained light grayish after sintering, possibly due to temperature gradients. The interior area is also slightly more porous than the exterior, as seen by the lower totals in this region (Table 1).

Fig. 8b and c shows the results from an EPMA line scan from Point 1 to 2 on the aggregate in Fig. 8a. The gap in the plots in Fig. 8b and c at 30 µm represents the crack at the paste–aggregate interface; points taken in this area are misleading and are therefore omitted. The lines for SiO_2 and the totals in Fig. 8b nearly overlap in the aggregate, indicating that the composition is almost entirely the original silica. When the *y*-axis scale is reduced (Fig. 8c), we can see that the small amount of calcium present inside the aggregate decreases quickly with distance from the paste–aggregate interface. The drop at 230 µm reflects a drop in the totals. The amount of calcium in the exterior region of these aggregates (2.8%; Table 1) is much lower than in the corresponding silica fume agglomerates (11%; Table 1). The amount of Na_2O inside the sintered silica fume aggregate is negligible (Fig. 8c, Table 1), as it was for the silica fume agglomerate.

3.3. ASR

Expansion test results are shown in Fig. 9a and b for sand- and limestone-containing mortars, respectively. The 100% sand samples expand more than 0.1–0.2% after 14 days under accelerated testing conditions, classifying the sand as a reactive aggregate. Sintered silica fume is clearly reactive, with an expansion of 0.7% after 14 days. On the other hand, all sizes of silica fume agglomerates considerably reduce expansion, with no significant differences between the sizes. The mortar bars made with limestone aggregates, with and without silica fume agglomerates, do not expand under the testing conditions. Not only are the agglomerates nonexpansive, they also reduce the expansion of reactive sand.

After the completion of the expansion tests, the two-toned appearance of the large agglomerates remains (Fig. 10a and b). The centers of the large agglomerates are

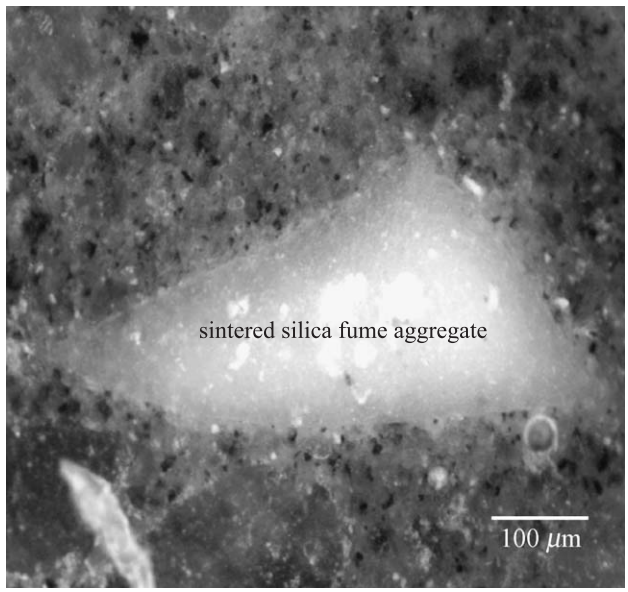

Fig. 7. Optical microscope image of a sintered silica fume aggregate in mortar after curing for 24 h at room temperature and 6 days at 80 °C.

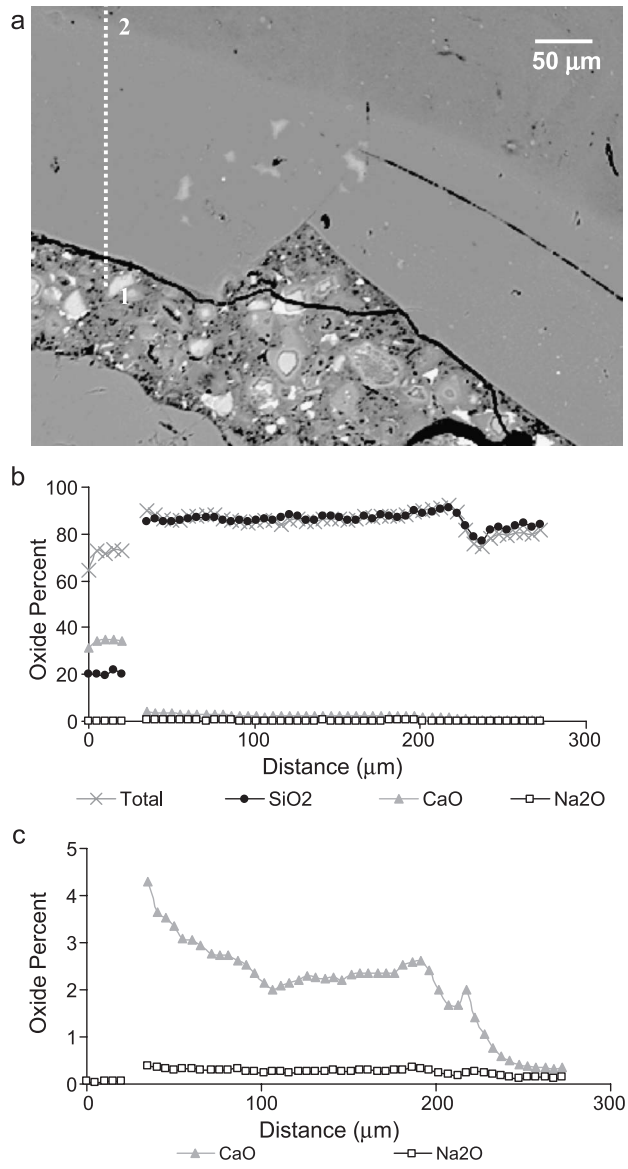

Fig. 8. (a) BSE image of a sintered silica fume aggregate in mortar after curing for 24 h at 20 °C + 6 days at 80 °C. (b) Elemental composition along the dotted line in Panel (a) from Point 1 to 2. (c) Same plot as in Panel (b), but with reduced *y*-axis scale.

slightly darker after NaOH exposure and are more uniform in texture; many remain hollow and some are cracked. There is no visible change in the smaller silica fume agglomerates (Fig. 10b). The sintered silica fume aggregates have clearly reacted under the testing conditions (Fig. 10c). This aggregate has a hollow center and a dense rim at the paste/aggregate interface; dense rims are characteristic of alkali silica gels in some natural aggregates. Further details on the reaction features of the sintered aggregates can be found in a previous publication [21].

Fig. 11 shows a BSE image of a silica fume agglomerate in mortar after 39 days of exposure to the NaOH solution, and an oxide analyses of the points taken across the agglomerate using EPMA. The boundary where the agglomerate ends and paste begins in Fig. 11b can be seen by the drop in silicon and sodium oxide concentrations and the rise in calcium oxide; the interfaces are marked by gaps in the plots. A reaction between the agglomerate and the paste has clearly taken place, as there are significant amounts of calcium and sodium inside the agglomerate, both of which are present in relatively constant concentrations throughout this particular agglomerate. From Table 1, it is clear that the amounts of calcium and sodium inside the agglomerates have increased appreciably after exposure to NaOH. Furthermore, the interior of the agglomerates has densified considerably. Not only is the interior more dense, on average, than before NaOH exposure (totals of 91% compared with 44%), but it is even denser than the exterior rim (82%). This is indicative a reaction between the agglomerates and the NaOH-containing pore solution, resulting in a reaction product that is denser than the original agglomerate.

Fig. 12 shows a BSE image and oxide analyses for a sintered silica fume aggregate after 39 days of exposure to NaOH. This aggregate has a hollow center and two clear rims, an outer dense one and an inner porous one. Within a given region, the amounts of SiO_2, Na_2O, and CaO do not vary much. Significantly more calcium and sodium are present in the aggregates after NaOH exposure than before exposure (Table 1). Comparing the amounts of calcium and sodium in the inner rim to the outer rim is problematic. It

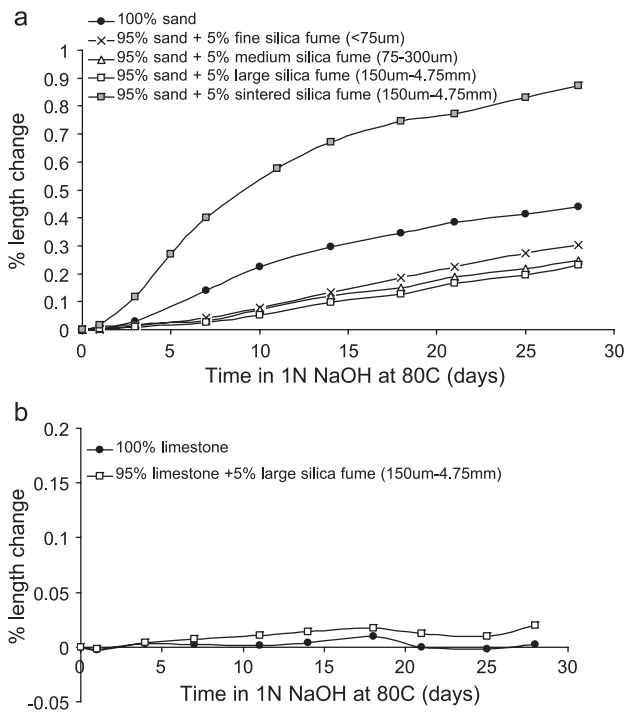

Fig. 9. Expansion of mortar bars in 1 N NaOH solution at 80 °C: (a) sand and (b) limestone.

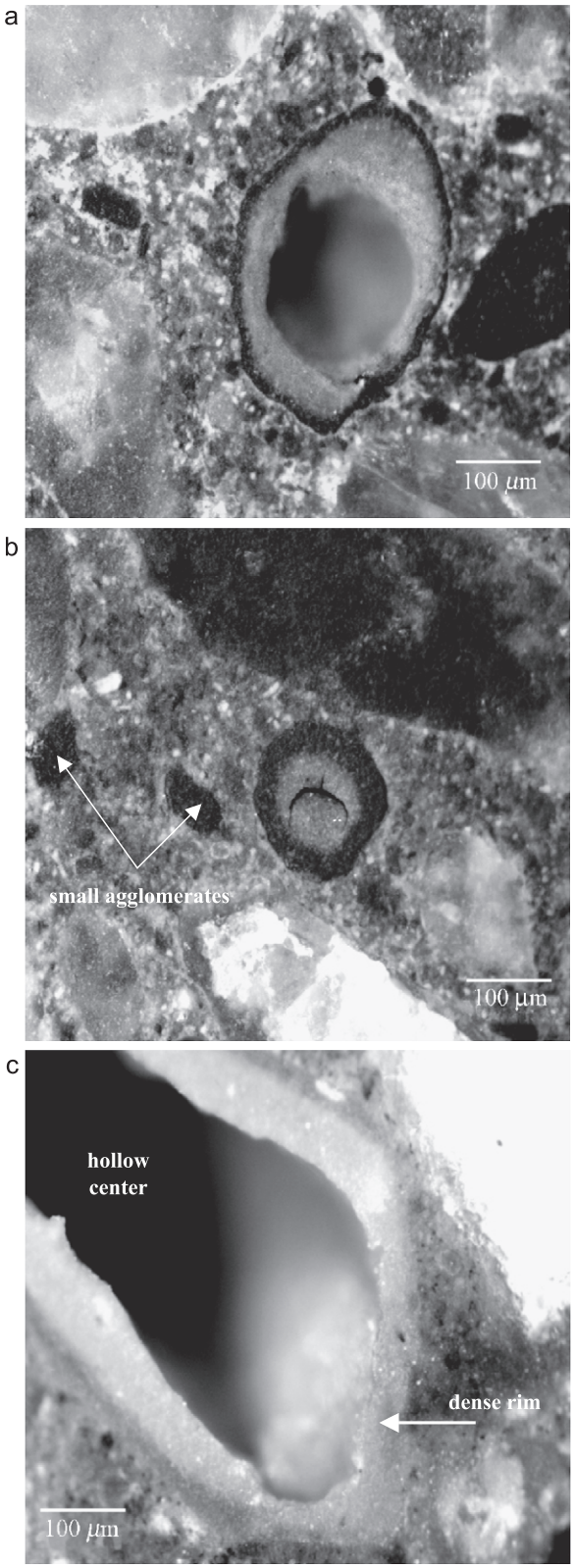

Fig. 10. Optical microscope images of silica fume-derived aggregates in mortar after 39 days in 1 N NaOH at 80 °C: (a) and (b) agglomerates, (c) sintered aggregate.

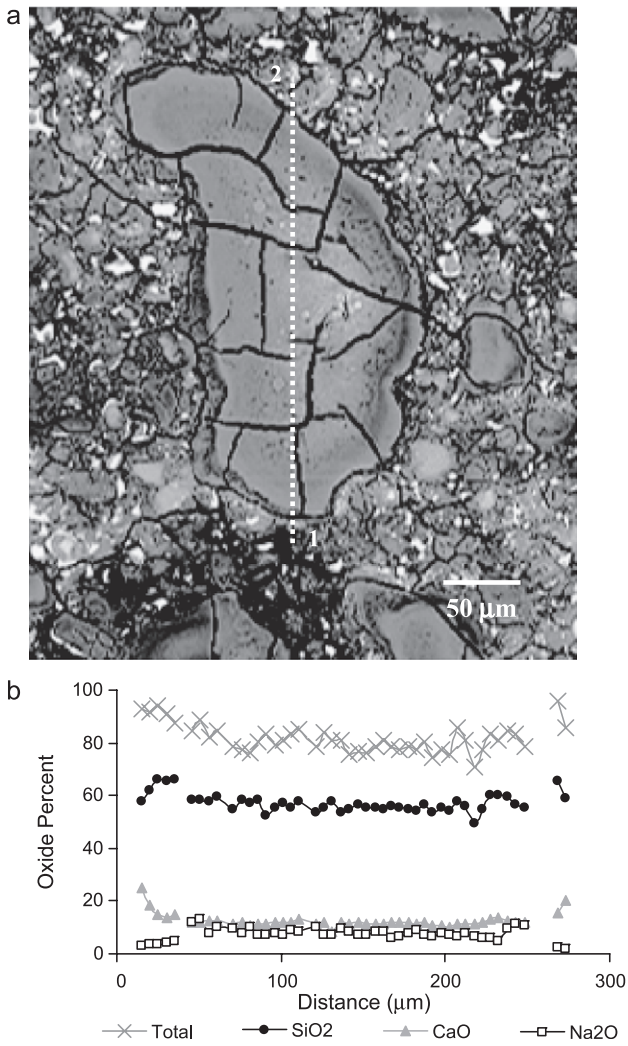

Fig. 11. (a) BSE image of a silica fume agglomerate. (b) Elemental composition along the dotted line in Panel (a) from Point 1 to 2.

appears from Fig. 12b and Table 1 that the inner rim has lower sodium and calcium concentrations than the exterior. The data are misleading, however, because the areas have different porosities. The oxide percents are calculated based on a total of 100% of the elements in a particular spot being detectable. In Fig. 12, an average of 95% of the elements in the outer rim is accounted for, but only 41% in the inner rim is accounted for. When the total is much less than 100%, the values are less reliable. The values for individual oxides are correlated with the total amount. This can be seen clearly in Fig. 12b: As the total value drops, so do all of the other values. In the pre-NaOH samples, we can directly compare the amounts of CaO, for example, in the interior and exterior because the totals are very similar. When the totals are widely different, it may be more appropriate to examine the ratios of elements (e.g., CaO/SiO_2). From Table 1, we can see that the average CaO/SiO_2 (C/S) ratio in the inner rim is slightly lower than that in the outer rim (average of 0.36 vs. 0.44) for the sintered aggregate. The silica fume agglomer-

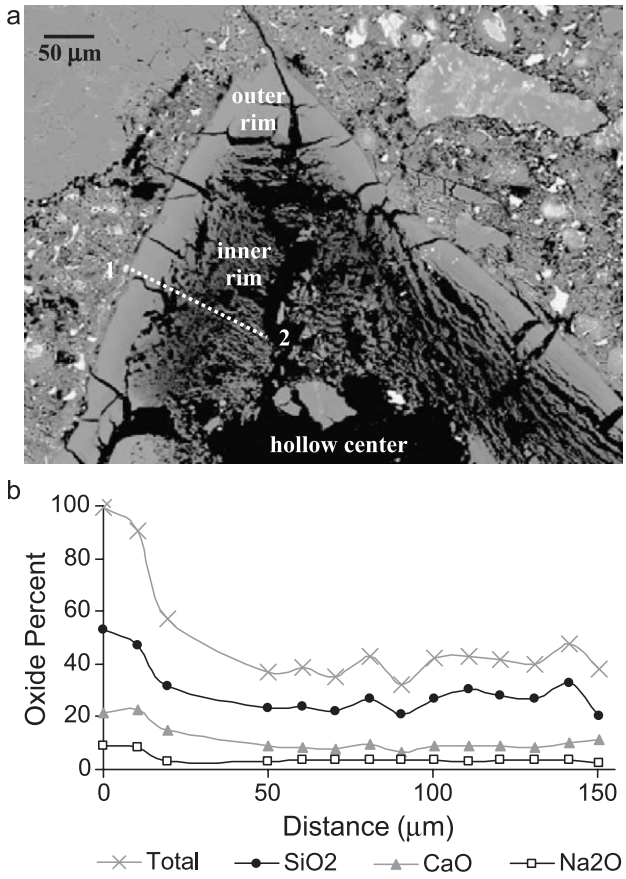

Fig. 12. (a) BSE image of a sintered silica fume aggregate. (b) Elemental composition along the dotted line in Panel (a) from Point 1 to 2.

ates have similar average C/S ratios (0.33 and 0.46) after exposure to NaOH.

4. Discussion

4.1. Silica fume characterization

It is likely that the dense outer rim seen in Fig. 1 is a result of the silica fume densification process. The close packing of the particles in the outside rim is responsible for the agglomerate maintaining its form. This morphology contrasts with that seen for densified silica fume by other researchers [5], some of who saw denser centers and looser outer rims. The differences in densification processes may account for these morphological variations. The morphology of the agglomerates is distinctly different from the sintered aggregates. While the former is a collection of loosely bound particles, the latter are continuous networks of bonded silica, with very few remaining spherical particles (Fig. 3).

The most striking microstructural feature of the silica fume agglomerates in mortar is their two-toned appearance after extended curing. The irregular texture of the centers of the agglomerates (including the hollow and porous features in Figs. 4 and 5) is probably a direct consequence of the fact that they are clusters of small particles and can easily dissolve and break apart during the polishing process. The coloration change may be related to a chemical reaction between the cement paste pore solution and the agglomerate. A reaction is evidenced by the presence of calcium within the agglomerates. There may be a limited reaction radius, accounting for the dark coloration of the small agglomerates and the two-toned appearance of the large ones. The two-toned characteristic may also be related to the original morphology of the agglomerates seen in Fig. 1; the dense outer rim darkens upon reaction with the pore solution.

The observation that silica fume agglomerates react with pore solution in low-alkali cement is not new. Our research confirms that of Bonen and Diamond [3], who found similar results for silica fume in a 1-year-old cement paste. They observed calcium within the siliceous particles, with the concentration decreasing continuously toward the center of the particles. Particles also existed with relatively calcium-rich rims and calcium-free cores. Their BSE images showed darker centers and lighter rims, similar to that in Fig. 6a, due to the decrease in calcium toward the center. The brightness in BSE images indicates a higher atomic number; in cement-based systems, this usually corresponds to a higher amount of calcium. Bonen and Diamond [3] also reported small amounts ($<3\%$) of Na_2O and K_2O within the agglomerates. Whereas their 1-year-old samples had C/S ratios approximating that of C–S–H, ours are much lower, perhaps, due to our shorter (yet accelerated) curing time.

The sintered silica fume particles are relatively nonreactive prior to expansion testing in mortars containing low-alkali cement. A minimal amount of calcium has diffused into the particles, with the highest concentration close to the paste–aggregate interface. The pore solution probably entered the aggregate through the discrete pores within the aggregate. These synthetic aggregates are much more porous than natural aggregates due to inhomogeneous sintering [21] and thus allow easier infiltration of pore solution.

4.2. Expansion

It is clear from Fig. 9 that the silica fume agglomerates used in this study do not cause alkali–silica-related expansion; in fact, they suppress it. The agglomerates are acting in the same manner as finely distributed silica fume. The most commonly discussed mechanisms for pozzolanic reduction of ASR expansion were listed in the Introduction. Of these, the reduction of alkalis in the pore solution by dilution of cement and/or increase in low-lime C–S–H production is the most accepted [1,18,19,23]. The theory that pozzolans reduce ASR expansion by dilution of the alkalis naturally present in cement, however, is not valid in this study. All samples had the same cement content because silica fume

was used as an aggregate replacement rather than as a cement replacement.

Even when using an accelerated test, where access to alkalis is unlimited (such as ASTM C1260), pozzolans decrease the pH of the pore solution during the 14-day period prescribed by the test [18]. With longer exposure times, pH increases as the NaOH from the immersion solution saturates the pore system. In this study, therefore, the most pertinent information can be gained by examining the differences in expansion during the early days (<14) of the test in Fig. 9a. As early as 3 days, the sintered silica fume samples diverge from the control samples, expanding rapidly. The sand is slower to react than the sintered silica fume. The agglomerated silica fume is able to suppress expansion as soon as the sand starts reacting at 7 days. The continuous, consistent expansion after 14 days is due to sand reacting with the excess of NaOH present in the accelerated test. It should be noted that the slopes of the expansion curves are similar for all of the samples after this point (samples were examined through 84 days), suggesting that the effects of silica fume, both sintered and agglomerated, become negligible. Theories as to why the agglomerates and aggregates behave so differently will be presented later in this discussion.

4.3. ASR morphology and composition

After exposure to the NaOH solution, the large agglomerates are still two-toned, but the interior is darker and denser (Fig. 10a and b, Table 1). The agglomerates have clearly reacted with the high-alkali pore solution, taking in sodium and more calcium and changing color. The reaction product of the agglomerates and the pore solution is denser than the original agglomerate (Table 1), but it must not exert an expansive pressure on the mortar, given the results in Fig. 9. The concentration of sodium inside the agglomerates is higher than in the surrounding paste (average of 2.4%, range of 0.60–5.2%). It is possible that these agglomerates are acting as "sodium sinks", capturing alkalis so that they cannot react with the sand during the early stages of the expansion test. One of the most accepted mechanisms suggested for the reduction of alkali–silica expansion by finely distributed pozzolans is that they lower the C/S ratio of C–S–H throughout the paste [23,24]. A lower C/S ratio in C–S–H facilitates the incorporation of alkali ions into its structure, removing them from the pore solution. In our case, the C/S ratio of the agglomerates is very low, much lower than C–S–H, suggesting that the agglomerates can act as sodium sinks, reducing the concentration of alkalis in the pore solution. The agglomerates are effective in retaining sodium although the samples used for EPMA were exposed to the NaOH bath for 39 days, longer than the validity of the expansion test. The potential reduction in pH caused by these sinks does not preclude reduction due to low lime C–S–H in the cement paste, as the two mechanisms can act simultaneously when fine silica fume is also present.

After exposure to NaOH solution, the sintered silica fume aggregates are characterized by hollow centers and a dense rim of alkali–silica gel near the paste (Figs. 10c, 12a). Dent Glasser and Kataoka [25] have shown that the total amount of silica that can dissolve depends on the alkali concentration of the surrounding solution. In this system, therefore, some of the silica goes into the solution while the rest must remain in solid form. The framework of the remaining solid silica is attacked by alkalis, and an expansive alkali–silica gel is formed. The solid rims in Figs. 10c and 12a are alkali–silica gel, and the hollow centers must have contained an alkali–silica fluid. When water is present, the gel expands, resulting in an osmotic pressure great enough to cause cracking in the cement paste matrix. The less dense inner rim is most likely an area where the silica is incompletely dissolved or reacted.

4.4. Pozzolanic versus alkali–silica reaction

The reason for the tremendous difference in expansive behavior of sintered and agglomerated silica fume is either physical or chemical in nature. It is known that increasing the porosity of the system (e.g., using air-entraining agents) reduces ASR expansion [26,27]. This is effective because the ASR gel expands into free pores, thus alleviating the pressure exerted by the gel, reducing cracking and expansion. Silica fume agglomerates are more porous than the sintered silica fume aggregates, and so they should certainly be less expansive. However, silica fume agglomerates are not simply less reactive than the sintered aggregates, they exhibit the opposite behavior—they inhibit expansion caused by natural sand. This phenomenon cannot be simply explained by a physical difference in porosity.

The differences in behavior in these particles may have its roots in the difference between the pozzolanic reaction and the alkali–silica reaction. These reactions are very similar in that OH^- ions from the high-pH pore solution attack Si–O–Si bonds, dissolving the amorphous silica network and leaving loose SiO^- pairs and fragmented networks in solution. The difference lies in the cations that balance these negatively charged groups. In the pozzolanic reaction, very small grains of amorphous silica are surrounded by a Ca^{2+}- and OH^--rich pore solution upon mixing and act as nucleation sites for CH. The pozzolanic particles have a very high surface area, with several sites open to be attacked by OH^- ions from the pore solution. When the silica network of a pozzolanic particle is broken down by hydroxyl ions, Ca^{2+} ions from the CH immediately surrounding the particle combine with the loosened silica groups, creating a form of C–S–H. C–S–H has a relatively rigid structure and is not expansive.

In the case of alkali–silica reactive aggregates, anions and cations must diffuse into the aggregate before reacting. This occurs rather slowly in natural systems, after much of the available Ca^{2+} ions are already bound into the cement hydration products, in contact only with the outer edge of

the aggregate. Therefore, free Na^+ and K^+ ions are more readily available to balance out SiO^- groups than Ca^{2+} ions do. The resulting alkali–silica gel is loosely structured and can imbibe water easily, causing expansion.

It has been shown that the higher the calcium-to-sodium (or potassium) ratio of an alkali–silica gel, the less expansive it is [28]. It is also known that for an alkali–silica gel to be expansive, it must contain some calcium [29–31]. The precise effect of the calcium-to-sodium ratio on expansion is not well understood and is controversial. The theory that follows is based on comparing the pozzolanic reaction to the alkali silica reaction, with the assumption that the former creates a calcium-rich gel and is nonexpansive, while the latter creates an expansive sodium-rich gel.

The agglomerated silica fume particles may maintain a pozzolanic-type behavior, similar to dispersed silica fume, while the sintered silica fume particles behave more like reactive, natural aggregates. Figs. 1–3 show SEM images of silica fume agglomerates and a sintered silica aggregate. In the agglomerates, the silica fume particles are densely packed (Fig. 1c and d). Many spherical, individual particles of silica are apparent. These are most likely held together by van der Waals forces. In Fig. 3, necks have formed between the silica fume particles by the sintering process, creating a dense, continuous silica matrix. Some discrete pores and errant particles remain due to inhomogeneous sintering [21].

The surface area of the agglomerate is necessarily much higher than that of the sintered aggregate. During mixing and curing, the calcium-rich pore solution can infiltrate the silica fume agglomerates and surround the individual silica fume particles more easily due to the high porosity (Fig. 13a). As hydroxyl ions begin to break down the silica framework, Ca^{2+} ions are readily available, and a gel begins to form. Under the accelerated testing conditions, this process was happening even before the introduction of NaOH, resulting in the dark rims seen in the optical images in Fig. 5. The gel that forms is not a true C–S–H, as the C/S ratio is too low. When silica fume is highly dispersed, each particle is surrounded by calcium-rich pore solution and calcium-rich cement grains; hence, there is plenty of calcium available to react with the silica. In a large agglomerate, silica is so locally concentrated that not enough calcium can come in from the pore solution to create a true C–S–H. The resulting product may exist either as an unknown phase with a very low C/S ratio, or as a mixture of true C–S–H and unreacted silica.

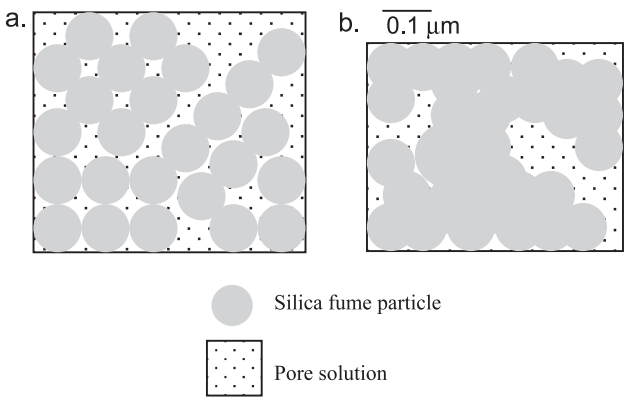

Fig. 13. Diagram of difference in contact area between silica fume particles in (a) an agglomerated particle and (b) a sintered particle.

Because the silica fume in the sintered aggregates has been densified and bonded, the initial pore solution can only penetrate discrete pores within the aggregate (Fig. 13b). The surface area is lower, and the hydroxyl ions must break down the silica framework before a reaction can happen anywhere other than on the pore surfaces. Once this occurs, alkali ions are more readily available to form an alkali–silica gel; the Ca^{2+} ions are already bound into the CH and C–S–H in the paste and are physically too far away from the reactive sites. The result is that the alkali–silica gel in the sintered aggregates is relatively calcium-poor from the beginning and, therefore, highly expansive. Conversely, the alkali–silica gel in the agglomerates is relatively calcium-rich in the beginning and thus nonexpansive.

In systems with natural reactive aggregates, the alkali ions in the alkali–silica gel are slowly replaced by calcium ions diffusing in from the pore solution, especially in cracks and at the paste–aggregate interface [32,33]. As this happens, the gel gradually becomes less expansive. The sintered aggregate-based gel incorporates calcium from the pore solution over time and ceases to expand, similar with natural aggregates. Over time, the agglomerate-based gel incorporates sodium from the solution, similar to a low C/S ratio C–S–H, becoming effectively a sodium sink, as described earlier. These processes result in steady-state gels with similar C/S ratios, as seen in Table 1. This explains the similar slopes of the expansion curves in Fig. 9a after 14 days for both types of aggregates. The sintered aggregates have stopped expanding because they have incorporated a critical amount of calcium into the gel product. The agglomerates cannot incorporate any more sodium, leaving the incoming NaOH from the pore solution free to react with sand. The rate of expansion after 14 days is equivalent in all systems because it is entirely dependent on the slowly reacting sand.

Inconsistencies in previous laboratory and field studies concerning the alkali–silica reactivity of large particles in silica fume may have to do with whether the particles were agglomerated or bonded. Some commercially available silica fumes have large, covalently bonded or fused silica particles [2]. These would contribute deleteriously to ASR. Other batches of silica fume, such as the one used in this study, reduce expansion despite the presence of large particles because these are truly clusters of smaller particles. The theory presented for why these two types of silica fume particles behave differently is based on controversial data in the literature. A better understanding for why these particles behave differently may be gained in the future as we learn more about the mechanisms of ASR. The observation remains, however, that expansive sintered silica fume has

a dense matrix of bonded silica, while expansion-reducing agglomerates are composed of loosely packed individual particles. The differences in the behavior of these two systems must be based on that fact, independent of the mechanism.

5. Conclusions

Large particles of silica fume may either decrease or increase expansion due to alkali–silica reaction in mortar. Under the accelerated testing conditions used in this study, agglomerated silica fume decreased expansion when used as a 5% replacement of reactive sand. When the same sand was replaced by 5% of sintered silica fume aggregates, expansion considerably increased. Both types of particles reacted with the pore solution in mortar. The difference in behavior is most likely related to the nature of the chemical reactions between the alkaline pore solution and the two types of particles.

Acknowledgements

The authors would like to thank C. Yi, J. Donovan, and T. Teague for their help with the experiments described herein. The comments and insight of P.J.M. Monteiro are also gratefully acknowledged. Funding for this research was provided by the National Science Foundation Grant No. CMS-962480.

References

[1] J. Duchesne, M.A. Bérubé, The effectiveness of supplementary cementing materials in suppressing expansion due to ASR: Another look at the reaction mechanisms: Part I. Concrete expansion and portlandite depletion, Cem. Concr. Res. 24 (1994) 73–82.
[2] D. Bonen, S. Diamond, Investigations on the coarse fraction of a commercial silica fume, Proceedings, 14th International Conference on Cement Microscopy, ICMA, Duncanville, TX, 1992, pp. 103–113.
[3] D. Bonen, S. Diamond, Occurrence of large silica fume-derived particles in hydrated cement paste, Cem. Concr. Res. 22 (1992) 1059–1066.
[4] G. Gundmundsson, H. Olafsson, Silica fume in concrete—16 years of experience in Iceland, Alkali-Aggregate Reaction in Concrete, Proceedings of the 10th International Conference, AARC Australia, Melbourne, 1996, pp. 469–562.
[5] R.D. Hooton, R.F. Bleszynski, A. Boddy, Issues related to silica fume dispersion in concrete, Materials Science of Concrete—The Sidney Diamond Symposium, American Ceramic Society, Westerville, OH, 1998, pp. 435–446.
[6] D.A. St. John, The dispersion of silica fume, in: K.L. Scrivener, J.F. Young (Eds.), Mechanisms of Chemical Degradation in Cement-based Systems, E & FN Spon, London, 1997, pp. 58–66.
[7] S. Diamond, S. Sahu, Densified silica fume—is it what you think it is? Proceedings of Advances in Cement and Concrete, IX, Copper Mountain, Colorado Department of Civil Engineering, University of Illinois, Urbana-Champaign in Urbana, Illinois, 2003, pp. 233–248.
[8] S. Diamond, Alkali silica reaction—some paradoxes, Cem. Concr. Compos. 19 (1997) 391–401.
[9] C. Perry, J.E. Gillott, The feasibility of using silica fume to control concrete expansion due to alkali–aggregate reactions, Durab. Build. Mater. 3 (1985) 133–146.
[10] A. Shayan, G.W. Quick, C.J. Lancucki, Morphological, mineralogical and chemical features of steam-cured concretes containing densified silica fume and various alkali levels, Adv. Cem. Res. 5 (20) (1993) 151–161.
[11] A. Shayan, G.W. Quick, C.J. Lancucki, Reactions of silica fume and alkali in steam-cured concrete, Proceedings of the 16th International Conference on Cement Microscopy, ICMA, Duncanville, TX, 1994, pp. 399–410.
[12] P.R. Rangaraju, J. Olek, Evaluation of the potential of densified silica fume to cause alkali–silica reaction in cementitious matrices using a modified ASTM C 1260 test procedure, Cem., Concr. Aggreg. 22 (2), pp. 150–159.
[13] K. Pettersson, Effects of silica fume on alkali–silica expansion in mortar specimens, Cem. Concr. Res. 22 (1992) 15–22.
[14] D.A. St. John, S.A. Freitag, Fifty years of investigation and control of AAR in New Zealand, Alkali-Aggregate Reaction in Concrete, Proceedings of the 10th International Conference, AARC Australia, Melbourne, 1996, pp. 150–157.
[15] S.L. Marusin, L.B. Shotwell, Alkali–silica reaction in concrete caused by densified silica fume lumps: a case study, Cem., Concr. Aggreg. 22 (2) (2000) 90–94.
[16] A.M. Boddy, R.D. Hooton, M.D.A. Thomas, The effect of product form of silica fume on its ability to control alkali–silica reaction, Cem. Concr. Res. 30 (2000) 1139–1150.
[17] ASTM C 1260-94, Standard test method for potential alkali reactivity of aggregates (mortar-bar method), Annual book of ASTM Standards v. 04.02 (Concrete and Aggregates), American Society for Testing and Materials, Philadelphia, 1999, pp. 650–653.
[18] M.A. Bérubé, J. Duchesne, D. Chouinard, Why the accelerated mortar bar method ASTM C 1260 is reliable for evaluating the effectiveness of supplementary cementing materials in suppressing expansion due to alkali–silica reactivity, Cem., Concr. Aggreg. 17 (1995) 26–34.
[19] M.D.A. Thomas, F.A. Innis, Use of the accelerated mortar bar test for evaluating the efficacy of mineral admixtures for controlling expansion due to alkali–silica reaction, Cem., Concr. Aggreg. 21 (1999) 157–164.
[20] L. Turanli, K. Shomglin, C.P. Ostertag, P.J.M. Monteiro, Reduction in alkali–silica expansion due to steel microfibers, Cem. Concr. Res. 31 (2001) 825–827.
[21] M.C.G. Juenger, C.P. Ostertag, Effect of selective positioning of steel microfibers on alkali–silica expansion, Concr. Sci. Eng. 4 (2002) 91–97.
[22] D.W. Hobbs, The alkali–silica reaction—a model for predicting expansion in mortar, Mag. Concr. Res. 33 (1981) 208–219.
[23] J. Duchesne, M.A. Bérubé, Effect of supplementary cementing materials on the composition of cement hydration products, Adv. Cem. Based Mater. 2 (1995) 43–52.
[24] M.S.Y. Bhatty, Mechanism of pozzolanic reactions and control of alkali–aggregate expansion, Cem., Concr. Aggreg. 7 (1985) 69–77.
[25] L.S. Dent Glasser, N. Kataoka, The chemistry of "alkali–aggregate" reaction, Cem. Concr. Res. 11 (1981) 1–9.
[26] W.J. McCoy, A.G. Caldwell, New approach to inhibiting alkali-aggregate expansion, J. Am. Concr. Inst. 22 (1951) 693–706.
[27] A.D. Jensen, S. Chatterji, P. Christensen, N. Thaulow, Studies of alkali–silica reaction: Part II. Effect of air-entrainment on expansion, Cem. Concr. Res. 14 (1984) 311–314.
[28] M. Prezzi, P.J.M. Monteiro, G. Sposito, The alkali–silica reaction: Part I. Use of the double-layer theory to explain the behavior of reaction-product gels, ACI Mater. J. 94 (1997) 10–17.
[29] M. Kawamura, N. Arano, T. Terashima, Composition of ASR gels and expansion of mortars, Materials Science of Concrete—The Sidney Diamond Symposium, American Ceramic Society, Westerville, OH, 1998, pp. 261–276.
[30] M. Kawamura, N. Arano, T. Terashima, Mechanisms of the sup-

pression of ASR expansion by fly ash from the view point of gel composition, Materials Science of Concrete—The Sidney Diamond Symposium, American Ceramic Society, Westerville, OH, 1998, pp. 277–284.
[31] M.D.A. Thomas, The role of calcium in alkali–silica reaction, Materials Science of Concrete—The Sidney Diamond Symposium, American Ceramic Society, Westerville, OH, 1998, pp. 325–337.
[32] T. Knudsen, N. Thaulow, Quantitative microanalyses of alkali–silica gel in concrete, Cem. Concr. Res. 5 (1975) 443–454.
[33] A.D. Buck, K. Mather, Alkali–silica reaction products from several concretes: Optical, chemical, and x-ray diffraction data, Proceedings of the 4th International Conference on the Effects of Alkalies in Cement and Concrete, Purdue University, W. Lafayette, IN, 1978, pp. 73–85.